Food Research International 172 (2023) 113100

Contents lists available at ScienceDirect

Food Research International

journal homepage: www.elsevier.com/locate/foodres

Lesser mealworm (*A. diaperinus*) protein as a replacement for dairy proteins in the production of O/W emulsions: Droplet coalescence studies using microfluidics under controlled conditions

Jitesh Jayakumar [a], Aurélie Ballon [a], Jordi Pallarès [b], Anton Vernet [b], Sílvia de Lamo-Castellví [a], Carme Güell [a], Montserrat Ferrando [a,*]

[a] Departament d'Enginyeria Química, Universitat Rovira i Virgili, Av. Països Catalans 26, 43007 Tarragona, Spain
[b] Departament d'Enginyeria Mecànica, Universitat Rovira i Virgili, Av. Països Catalans 26, 43007 Tarragona, Spain

ARTICLE INFO

Keywords:
Insect protein
Oil-in-water emulsion
Microfluidics
Droplet coalescence
Emulsion stability

ABSTRACT

Dairy proteins are commonly used to stabilize oil-in-water (O/W) emulsions, which can be replaced by other sustainable sources of proteins, such as insects. This study investigated the potential of lesser mealworm protein concentrate (LMPC) as a sustainable alternative to whey protein isolate (WPI) in stabilizing oil-in-water (O/W) emulsions using microfluidics. The frequency of coalescence (F_{coal}) was calculated using images of emulsion droplets obtained near the inlet and outlet of the coalescence channel. The stability of O/W emulsions, produced using sunflower oil (SFO) or hexadecane and stabilized with varying concentrations of LMPC and WPI (0.02% to 0.0005% w/v), was compared under controlled conditions. The dispersed phase fraction (5.3%-14.3% v/v), protein adsorption time onto oil droplets (0.0398–0.158 s), and pH (pH = 3 and pH = 7) were also studied. F_{coal} was greatest (0.42 s^{-1}) when the protein concentration was lowest (0.0005%), the oil percentage was highest (14.3%), the adsorption period was shortest (0.0398 s), and the pH was 3. Droplet diameters did not vary significantly, with values between 55 and 118 μm, across protein concentrations or adsorption periods, but a rise in oil fraction resulted in a substantial increase in droplet diameters. Increases in protein content, adsorption duration, and oil percentage all resulted in increased stability (reduction of F_{coal}). While LMPC and WPI showed similar results in microfluidic experiments and other test conditions, further research is needed to verify LMPC's efficacy as a replacement for WPI in food emulsification. Nonetheless, the findings suggest that LMPC has potential as a substitute for WPI in this application.

1. Introduction

The need for alternative protein sources which are more efficient and sustainable than animal proteins is widely acknowledged based on the need to deal with the expected protein demand in the upcoming years (Henchion, Hayes, Mullen, Fenelon, & Tiwari, 2017). Therefore, there is an increasing interest to assess the techno-functional properties of the new protein sources to facilitate their use in food applications (Henchion, Hayes, Mullen, Fenelon, & Tiwari, 2017; Yi & Boekel, 2013). Dairy proteins, with the ability to stabilize emulsions, are widely used by the food industry, and are within the group of proteins that may benefit from finding replacements amongst the new more sustainable protein sources. Edible insects are a novel source of proteins, reporting a protein content between 31 and 65% (Rumpold & Schlüter, 2013). Multiple publications point out towards insect proteins as a good replacement for dairy proteins as emulsifiers in food applications (Gould & Wolf, 2018; Kim et al., 2021; Mintah & Ma, 2020). Research carried out with protein extracts obtained from *S. gregaria* and *A. mellifera* had emulsifying capacities comparable to that of whey protein (Mishyna, Martinez, Chen, & Benjamin, 2019). An investigation into the emulsification properties of a protein concentrate from black soldier fly (*H. illucens*) to produce O/W emulsions using low-energy high-throughput emulsification technology showed that black soldier fly proteins could be a sustainable source of proteins in the food industry (Wang et al., 2021b). Moreover, lesser mealworm (*A. diaperinus*) protein concentrate, LMPC, was used to stabilize encapsulated polyphenols in a water-in-oil-in-water (W/O/W) emulsions showing that this protein was able to stabilize the emulsion similarly to whey protein and pea protein (Wang et al., 2021a).

* Corresponding author.
E-mail address: montse.ferrando@urv.cat (M. Ferrando).

https://doi.org/10.1016/j.foodres.2023.113100
Received 28 March 2023; Received in revised form 29 May 2023; Accepted 9 June 2023
Available online 10 June 2023

Emulsions are a mixture of two or more immiscible liquids, with one phase dispersed into the other as small spherical droplets (McClements, 2016). Emulsification includes droplet breakup, creating a new interface around the dispersed drops, and the stabilization of this interface with the use of emulsifiers to prevent demulsification. During emulsion production, droplet formation occurs simultaneously with droplet coalescence. Coalescence depends on the number of collisions per unit time and the efficiency of those collisions. The number of collisions is favored by droplet volume fraction, the sizes and spatial distribution of droplets, and the flow conditions, while the efficiency of the collisions relies upon the incomplete adsorption of emulsifiers on the droplet surface, and the resistance of the thin film material separating the droplets (Jafari, Assadpoor, He, & Bhandari, 2008; McClements, 2004; Yonguep, Kapiamba, Kabamba, & Chowdhury, 2022). The droplets, which completely adsorb the emulsifier on their interface, remain stable for a few seconds to months depending on several parameters, such as the type of emulsifier, kinetics of adsorption, temperature, pH, droplet size, and fraction of dispersed phase (Jafari, Assadpoor, He, & Bhandari, 2008; Narsimhan & Goel, 2001; Tcholakova, Denkov, & Banner, 2004).

During emulsification, the adsorption of emulsifier on the interface and the coalescence of droplets occur instantaneously within a span of few milli seconds, making it difficult to understand the dynamics of coalescence (Muijlwijk & Schroën, 2017). To do so, microfluidic devices enable to observe individual droplets and determine emulsion stability under carefully controlled conditions (Ho, Razzaghi, Ramachandran, & Mikkonen, 2022). Microfluidic devices have already been used in emulsion stability studies in both food and non-food applications. Emulsions are produced using different microfluidic emulsification systems, such as shear-driven droplet breakup systems (T-junction, co-flow, and focus-flow) or the ones based on Laplace pressure difference, known as the spontaneous emulsification systems (Maan, Nazir, Khan, Boom, & Schroën, 2015). Shear-driven emulsification has been extensively used for the preparation of single and multiple emulsions (Okushima, Nisisako, Torii, & Higuchi, 2004; Xu, Li, Tan, Wang, & Luo, 2006), and also to precisely control droplet size (Huang et al., 2020). It has also been used to determine the impact of operating conditions and emulsion formulation on the progress of the emulsifier adsorption at the interface, a determining step on emulsion stability. Some of these studies include determining the coalescence of emulsions stabilized with proteins (Muijlwijk & Schroën, 2017), the effect of oxidation of protein on droplet coalescence (Hinderink, Kaade, Sagis, Schroën, & Berton-Carabin, 2020), and determining the effect of elevated temperature on droplet coalescence (Bera, Khazal, & Schroën, 2021). Their results point out that the frequency of coalescence increases with the decrease in the protein concentration, the decrease in adsorption time, and the total flowrate of the emulsion (Dudek, Fernandes, Helno Herø, & Øye, 2020; Hinderink, Kaade, Sagis, Schroën, & Berton-Carabin, 2020; Muijlwijk & Schroën, 2017).

When proteins are used to stabilize emulsions, they exhibit different emulsifying properties depending on their nature and environmental conditions, such as pH, ionic strength, concentration of protein, and oil fraction, to name a few. Since microfluidics is an appropriate technology for learning about the effectiveness of novel protein sources as a substitute for dairy proteins to stabilize emulsions, the main objective of the current study is to evaluate the coalescence stability of model (hexadecane) and food grade (sunflower oil) O/W emulsions stabilized with lesser mealworm protein concentrate under controlled conditions. Using a custom-designed microchip, the effects of protein content, oil type, and fraction, as well as protein adsorption duration, are investigated. Moreover, a tailor-made image analysis methodology allows to account for droplet coalescence from the start of the coalescence channel by considering droplets of different sizes (dimers, trimers, and tetramers), calculate their rate of formation, and stablish the predominant coalescence dynamics. Additionally, the outcomes are compared with those attained under the same experimental settings with O/W emulsions stabilized with whey protein isolate, which is frequently employed as a reference system in food applications. This is the first attempt, as far as we are aware, to investigate the coalescence of an insect protein stabilized emulsion over short time scales under controlled conditions.

2. Materials and methods

2.1. Protein extraction and sample preparation

Lesser mealworm powder provided by Kreca, with a protein content of 48% (Kreca Ento-Food BV, Wageningen, the Netherlands) was mixed with 2-methyltetrahydrofuran (Scharlab S.L., Spain) in the ratio of 1:5 (w/w) and stirred under the hood at 600 rpm for 1 h. The solution was left to settle before decanting the solvent. This process was repeated to remove the fat from the insect powder. The left-over solvent with the insect powder in the beaker was left under the hood for it to evaporate. The obtained powder was then mixed with 0.25 M NaOH (Chem-Lab NV, Zedelgem, Belgium) and stirred at 40 °C for 1 h. The sample was centrifuged at 4500 rpm for 10 min and then the supernatant was carefully removed. The supernatant was mixed with 35% HCl (J.T. Baker, Griesheim, Germany) until the pH was set to 4.2. This solution was again subjected to centrifugation at 3800 rpm for 15 min. The process of extraction with NaOH and pH adjustment with HCl was repeated 2 more times to get the maximum extraction yield of the protein. The final obtained precipitate was freeze-dried to get lesser mealworm protein concentrate, (LMPC) with a protein content of 71% (wb). The protocol for the extraction of protein was referred from (Wang et al., 2021b).

Protein solutions were prepared in phosphate buffer with di-sodium hydrogen phosphate dihydrogen (Scharlau, Spain) and sodium phosphate monobasic monohydrate (ACROS, Spain) at pH = 7 and pH = 3 at concentrations of 0.02%, 0.01%, 0.005%, 0.001% and 0.0005% (w/w). Whey protein isolate (WPI), purchased from Davisco Foods International, Inc. (97.6%, Lot.JE151-4–420, Eden Prairie, MN, USA) with a reported protein content of 98.1% on dry basis was used to prepare the protein solution by directly weighing the required amount of protein powder to get the desired concentration. In the case of LMPC, a stock protein solution was prepared, and the concentration was determined using BCA (bicinchoninic acid) assay kit (Pierce Biotechnology, Thermo Scientific, Rockford, IL, USA). The stock solution was further diluted to the desired concentrations. These protein solutions were later used to stabilize the emulsions produced with hexadecane (purchased from Merck Germany) and sunflower oil (SFO) purchased from a local supermarket (Borges S.A., Tarragona, Spain).

2.2. Microfluidic set-up

Custom-designed microchips made of borosilicate glass were used for the microfluidic experiments (Micronit Microfluidics BV, The Netherlands). The microchip design comprises of two channels with rectangular cross-sections, the adsorption channel and the coalescence channel, and a T-junction (Fig. 1). The T-junction breaks down the dispersed phase into small droplets that flow through the adsorption channel without coming into contact with the other droplets, where protein from the continuous phase adsorbs to the oil–water interface. The droplets are then released into the coalescence channel, where they collide and may coalesce. The adsorption channel length was varied (14 mm and 20.5 mm) to determine the impact of protein adsorption time on droplet coalescence. The chip's channels had a fixed height of 45 μm and a width of 100 μm for the adsorption channel and 500 μm for the coalescence channel, and length of 32.1 mm for the coalescence channel.

Microfluidic emulsions were produced by mounting microchips on a microscope stage (Darwin Microfluidics, Paris, France) and connecting them to an Elveflow OB1 MK3 + pressure controller (ElveFlow, Paris, France), which controlled liquid flow rates. The continuous and

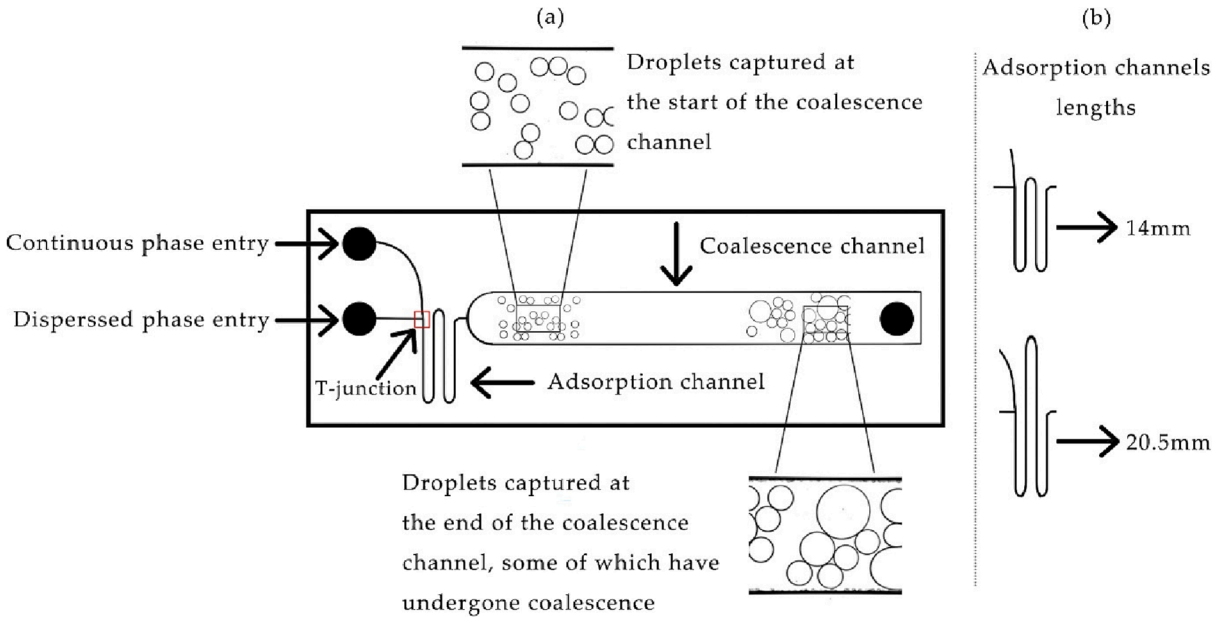

Fig. 1. (a) Outline of the microfluidic chip showing the different regions of the microchip and (b) lengths of adsorption channels used during experiments.

dispersed phases were pumped through a reservoir using compressed air, and a flow sensor provided feedback signals to keep the flowrate stable. Fig. 2 depicts the experimental setup.

2.3. Emulsion production and image acquisition

The oil and protein solutions were pumped at different total flowrates to generate emulsions with SFO (45 μl/minute to 105 μl/min) and hexadecane (35 μl/minute to 95 μl/min). The flowrate of the dispersed phase was kept constant at 5 μl/min while the flowrate of continuous phase was varied to attain the desired total flowrate and oil fraction. Droplet breakup at the T-junction was caused by the higher flowrate of the continuous phase, and the emulsion droplets then passed through the adsorption channel, where emulsifier adsorption at the surface of oil droplets may occur. Due to SFO's higher viscosity, droplet breakup at the T-junction did not occur at low flowrates, limiting the minimum total flowrate to 45 μl/min. The emulsion then entered the coalescence channel where droplets were free to collide with other droplets. A high-speed camera (SpeedCam MacroVis EoSens, Germany) was used to capture 500 images near the inlet and outlet of the coalescence channel (Fig. 1), and the images were processed using MATLAB. The experiments were conducted in duplicates, and the frame rate of the camera was varied according to the flowrate. Because of this, the number of images used to analyze droplet coalescence was varied accordingly to keep a constant experimental acquisition time of 10 s. Table 1 presents all the experimental conditions used.

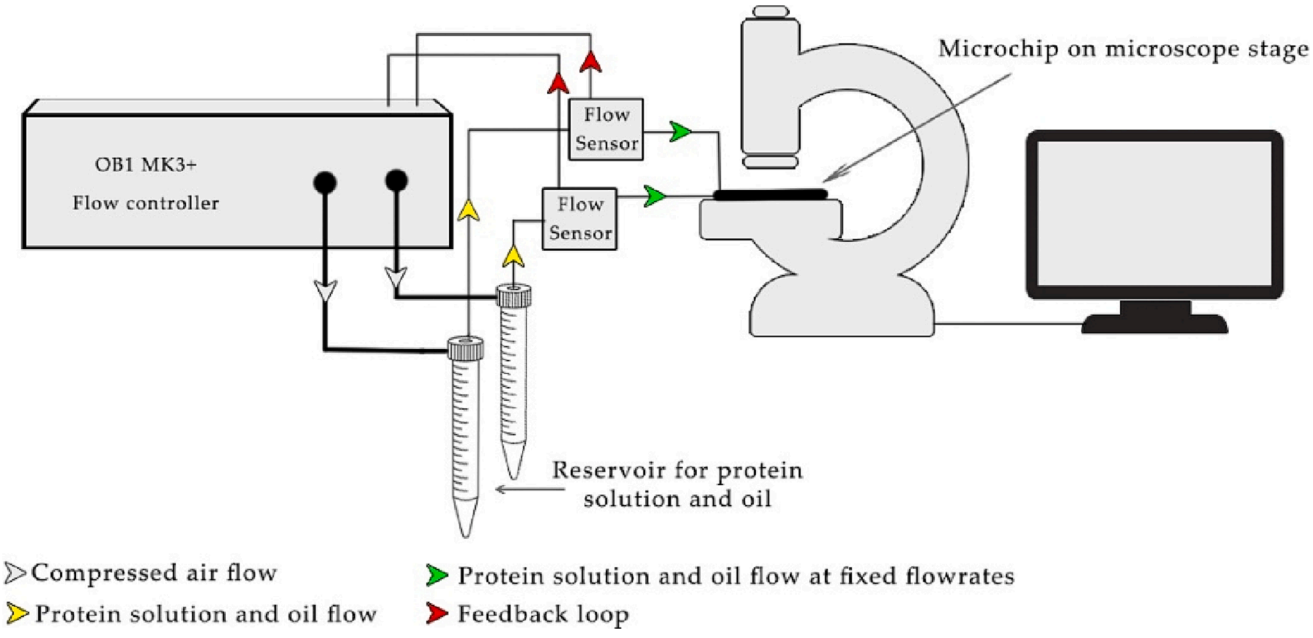

Fig. 2. Outline of the microfluidics experimental setup.

Table 1
Experimental conditions used to study emulsion stability using WPI and LMPC of hexadecane and sunflower oil emulsions.

Length of the adsorption channel	Water phase		Disperse phase		Total flow rate [μl/min]	Residence time	
	Emulsifier	pH	Oil type	Oil Fraction		Adsorption channel [s]	Coalescence channel [s]
14 mm	WPI	3 and 7	Hexadecane	14.3%	35	$1.08{\cdot}10^{-1}$	$9.64{\cdot}10^{-1}$
				7.7%	65	$5.82{\cdot}10^{-2}$	$5.19{\cdot}10^{-1}$
				5.3%	95	3.9810^{-2}	$3.55{\cdot}10^{-1}$
		7	Sunflower oil	11.1%	45	$8.42{\cdot}10^{-2}$	$7.52{\cdot}10^{-1}$
				7.7%	65	$5.82{\cdot}10^{-2}$	$5.19{\cdot}10^{-1}$
				5.3%	95	$3.98{\cdot}10^{-2}$	$3.55{\cdot}10^{-1}$
	LMPC	3 and 7	Hexadecane	14.3%	35	$1.08{\cdot}10^{-1}$	$9.64{\cdot}10^{-1}$
				7.7%	65	$5.82{\cdot}10^{-2}$	$5.19{\cdot}10^{-1}$
				5.3%	95	$3.98{\cdot}10^{-2}$	$3.55{\cdot}10^{-1}$
		7	Sunflower oil	11.1%	45	$8.42{\cdot}10^{-2}$	$7.52{\cdot}10^{-1}$
				7.7%	65	$5.82{\cdot}10^{-2}$	$5.19{\cdot}10^{-1}$
				5.3%	95	$3.98{\cdot}10^{-2}$	$3.55{\cdot}10^{-1}$
20.5 mm	WPI	3 and 7	Hexadecane	14.3%	35	$1.58{\cdot}10^{-1}$	$9.64{\cdot}10^{-1}$
				7.7%	65	$8.52{\cdot}10^{-2}$	$5.19{\cdot}10^{-1}$
				5.3%	95	$5.83{\cdot}10^{-2}$	$3.55{\cdot}10^{-1}$
		7	Sunflower oil	11.1%	45	$1.23{\cdot}10^{-1}$	$7.52{\cdot}10^{-1}$
				7.7%	65	$8.52{\cdot}10^{-2}$	$5.19{\cdot}10^{-1}$
				5.3%	95	$5.83{\cdot}10^{-2}$	$3.55{\cdot}10^{-1}$
	LMPC	3 and 7	Hexadecane	14.3%	35	$1.58{\cdot}10^{-1}$	$9.64{\cdot}10^{-1}$
				7.7%	65	$8.52{\cdot}10^{-2}$	$5.19{\cdot}10^{-1}$
				5.3%	95	$5.83{\cdot}10^{-2}$	3.5510^{-1}
		7	Sunflower oil	11.1%	45	$1.23{\cdot}10^{-1}$	7.5210^{-1}
				7.7%	65	$8.52{\cdot}10^{-2}$	5.1910^{-1}
				5.3%	95	$5.83{\cdot}10^{-2}$	3.5510^{-1}

2.4. Image analysis and calculation

The obtained images were analyzed with an in-house MATLAB script to determine the number and area of droplets. The frequency distribution of droplet area was determined using excel spreadsheet to distinguish between uncoalesced and coalesced droplets. The formation of dimers (two droplets merged to form a single droplet) and trimers (three droplets merged to form a single droplet) was identified by observing the doubling and tripling of the droplet area, respectively. Since microfluidics helps in producing monodispersed droplets, the dimers, trimers, and tetramers could be seen to exactly have double, tripled, or quadrupled in area than that of uncoalesced droplets. Fig. 3 shows the process flowchart of image analysis. The fraction of droplets undergoing coalescence (Dc) was calculated by using equation (1).

$$Dc = \frac{[(N2e*2) + (N3e*3) + \cdots.. + (Nne*n)]}{[N1e + (N2e*2) + (N3e*3) + \cdots.. + (Nne*n)]} - \frac{[(N2s*2) + (N3s*3) + \cdots.. + (Nns*n)]}{[N1s + (N2s*2) + (N3s*3) + \cdots.. + (Nns*n)]} \quad (1)$$

Where, N_{1e} and N_{1s} are the numbers of uncoalesced drops at the end and start of the coalescence channel respectively, N_{2e} and N_{2s} are the number of dimers at the end and start of the coalescence channel respectively. The frequency of coalescence was calculated using Equation (2).

$$Fc = \frac{Dc}{R} \quad (2)$$

Where, R is the residence time of droplets in the coalescence channel (Table 1). Residence time was calculated using the known volumetric

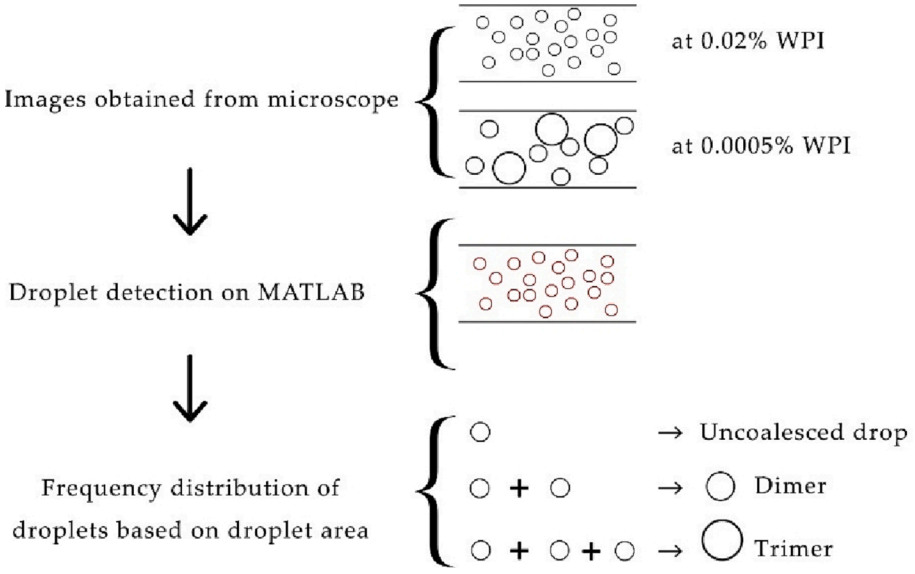

Fig. 3. Flowchart of the process of image analysis.

flowrates. The residence time in the adsorption channel was computed considering the total length of the adsorption channel, *Rt*, (14 or 20.5 mm) and the residence time in the coalescence channel was calculated between the start and end of the coalescence channel (2.5 cm in length), corresponding to the regions where images were taken.

2.5. Interfacial tension measurement

Interfacial tension was measured with Sigma T702-D (Biolin scientific, Sweden) by using the hanging ring method. The protein solution was taken in a beaker and placed on the stage. A platinum ring cleaned with ethanol, distilled water, and finally subjected to flame to get rid of all the impurities was hung on a hook and then slowly immersed into the liquid in the beaker. Oil was then slowly poured on the protein solution using a Pasteur pipette and the system was then left idle for the liquids to come to equilibrium (1 min). Interfacial tension was determined by the amount of energy required by the ring to break the interfacial strength and considers the difference in the density of the two liquids.

2.6. Statistical analysis

GraphPad was utilized to perform a one-way analysis of variance (ANOVA) to analyze the data. Significant differences were determined using ANOVA and Tukey test ($p < 0.05$). The data described are mean ± standard deviation.

3. Results and discussions

In this section, we will discuss the influence of various factors on the coalescence of emulsion droplets stabilized with proteins. Specifically, we will compare the efficacy of LMPC and WPI as emulsifiers. The microfluidic device utilized in this study allowed for precise control of droplet formation at T-junction, emulsifier adsorption time to the newly formed interface, and droplet stability at the coalescence channel, allowing a thorough investigation of the effect of operating conditions and emulsion formulation on droplet coalescence.

3.1. Droplet formation and emulsifier adsorption

3.1.1. Diameter of single droplets

Droplet areas obtained from MATLAB in pixels were converted to area in micrometers using ImageJ (Rasband, W.S., ImageJ, U. S. National Institutes of Health, Bethesda, Maryland, USA). Using the known area of the droplets, the average droplet diameter was calculated for the non-coalesced droplets. For constant process conditions, we should note that the average size of single droplets remains relatively invariable, with a range of standard deviation between 0.2 and 1 μm, what is below of 1.2% of variation and shows that emulsions are actually monodisperse. Fig. 4 presents the average size of hexadecane droplets near the inlet of the coalescence channel. It can be observed that the droplet size does not show a big variation at different protein concentrations, regardless of the protein used to stabilize the hexadecane emulsion. This was also found by Hinderink, et al., (2020) when studying the coalescence of hexadecane emulsions stabilized with pea protein. They also established that the initial droplet size was almost independent of the initial protein concentration, which can be related to a constant apparent interfacial tension during droplet formation. This could also be the case in the present situation for WPI and LMPC hexadecane stabilized emulsions.

From Fig. 4 it is also possible to observe the effect of the oil fraction and the pH on the initial droplet size of hexadecane emulsions stabilized with WPI and LMPC. Regardless of the protein there is a significant

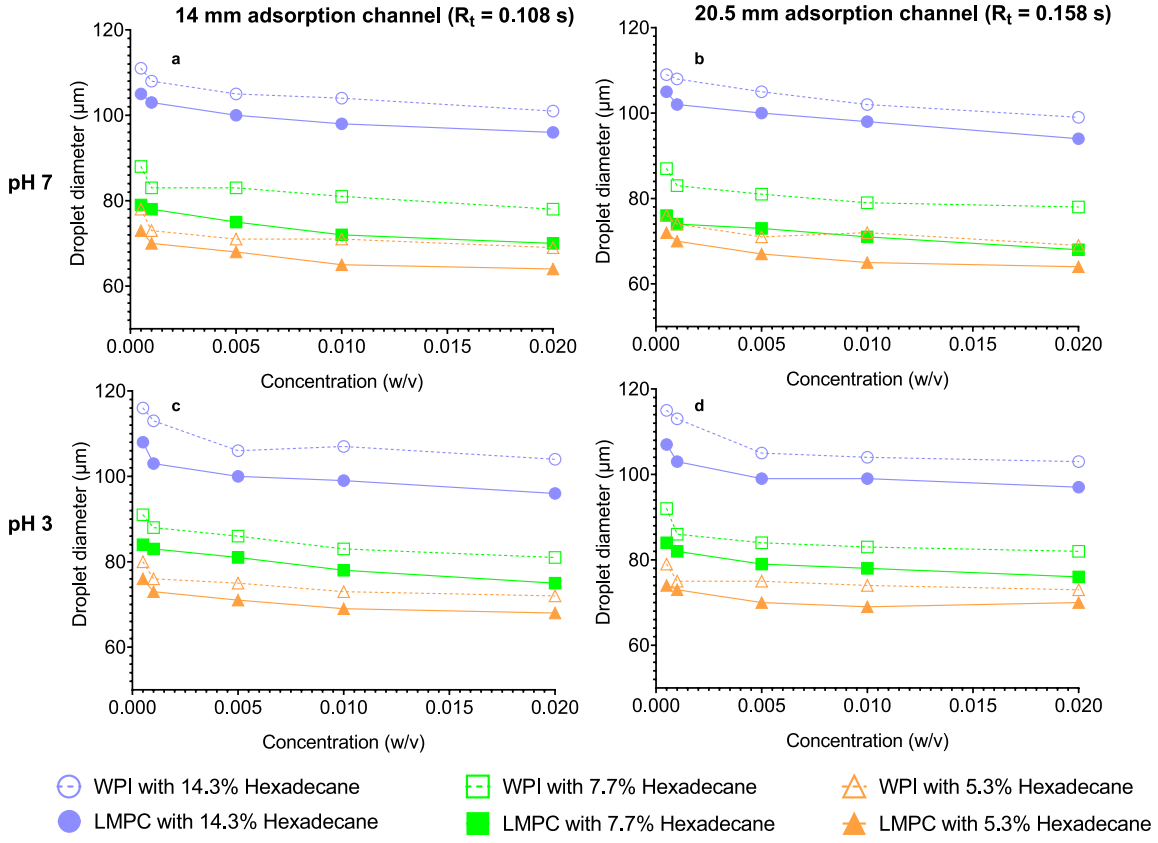

Fig. 4. Diameter of hexadecane droplets at different concentrations of WPI and LMPC. (a) pH 7 and 0.108 s adsorption time, R_t, (b) pH 7 and 0.158 s Rt, (c) pH 3 and 0.108 s R_t, and (d) pH 3 and 0.158 s R_t. Error bars showing standard deviation cannot be seen since they are smaller than the symbol size (range of the standard deviation from 0.2 to 1 μm).

increase in the droplet size with the increase in the oil fraction. Oil fraction is the highest when the flowrate of the continuous phase is at its lowest. Because of this low flowrate, the shear stress produced at the T-junction to break the oil droplet is lower, leading to the formation of bigger oil droplets. As for the acidic pH studied (pH = 3), the increase in the droplet size can be attributed to the conformation changes of the proteins under this environment leading to a decrease in the surface hydrophobicity, and also to the higher interfacial tension of the protein at pH 3 (Fig. 5). It can also be observed that the LMPC produces smaller droplets as compared to WPI (Fig. 4) for all the conditions studied. This could be explained because of the lower equilibrium interfacial tension between hexadecane and LMPC solution as shown in Fig. 5 that could be attributed to a higher molecular flexibility of this protein (Gould & Wolf, 2018).

SFO droplet size follows the same trends as for the hexadecane emulsions, showing a significant increase in droplet diameter with the increase of oil phase and a marginal increase in droplet diameter with a decrease in protein concentration (Figure S1, Supplementary material). SFO emulsions stabilized with LMPC also exhibit a slightly lower droplet size than the ones stabilized with WPI. Even though the interfacial tension of the two proteins with SFO is significatively lower than with hexadecane (Fig. 5), the reduction of droplet size does not shift accordingly, which could also indicate that droplet size is mainly governed by the flowrate of dispersed and continuous phases when the emulsion is produced using a T-junction microfluidic system. This can be observed while comparing the effect of the adsorption channel length on the droplet size. The droplet size remained constant despite the variation in the channel length used. Moreover, it has been reported that the apparent interfacial tension measured in the microchannels was not influenced by the bulk protein concentration. It was found that Tween 20 had a higher apparent interfacial tensions when compared to proteins (whey protein and bovine serum albumin), although the equilibrium interfacial tension of Tween 20 was lower than that of the proteins (Güell, Ferrando, Trentin, & Schroën, 2017).

Interfacial tension measurements are aligned with the fact that the flowrate and microchip design play a vital role in determining the droplet size for these systems. In conventional emulsification techniques, an increase in interfacial tension leads to bigger droplets and hence influencing the droplet diameter (McClements, 2004). But in the case of microfluidics, even though there is a clear increase in interfacial tension with the decrease in protein concentration, the droplet size increases only marginally. Fig. 5 shows the equilibrium interfacial tension between hexadecane/SFO and WPI/LMPC protein solutions at different concentrations of protein at pH = 3 and pH = 7. It can be observed that LMPC tends to reduce the interfacial tension more than WPI at both pH = 3 and pH = 7. SFO used as the oil phase reduces the interfacial tension drastically when compared to interfacial tension with hexadecane in the oil phase, and hence smaller droplet sizes could be expected for SFO emulsions than for hexadecane ones. In terms of molecular structure, hexadecane is an aliphatic long-chain saturated hydrocarbon. In contrast, sunflower oil is a complex mixture of triglycerides composed of glycerol and various unsaturated fatty acids (Akkaya, 2018; Camin, Forziati, & Rossini, 1964) which influence the interfacial behavior of oil molecules with proteins at the oil–water interface. The double bonds of unsaturated fatty acids give flexibility to their molecular structure, allowing them to more readily interact with proteins (Watanabe, Kawai, & Nonomura, 2018), and explaining the lower interfacial tension when compared to hexadecane. It has also been reported that in shear driven systems, such as T-junctions, a higher viscosity of the dispersed phase results in larger droplets. However, in the present study the combined effect of the interfacial tension and the flowrate overcome the effect of the higher SFO viscosity (49.19 mPa.s) compared to hexadecane (3.005 mPa.s).

3.1.2. Effect of pH, adsorption time, and oil fraction on the number of droplets undergoing coalescence at the start of the coalescence channel

By analyzing the droplets near the inlet of coalescence channel, it was clear that some droplets underwent coalescence immediately after getting released into the coalescence channel. By determining the number of droplets undergoing coalescence as soon as they leave the adsorption channel, the effect of adsorption time, pH, type and fraction of oil, and protein type and concentration on droplet stability could be measured. Fig. 6 presents the number of coalesced droplets as a function of these parameters at different protein concentrations for hexadecane. Protein concentration plays a major role in influencing droplet coalescence. Irrespective of the pH, oil type and fraction, and adsorption time, there is a considerable increase in the number of droplets undergoing coalescence to form dimers, trimers, and tetramers, with the decrease in

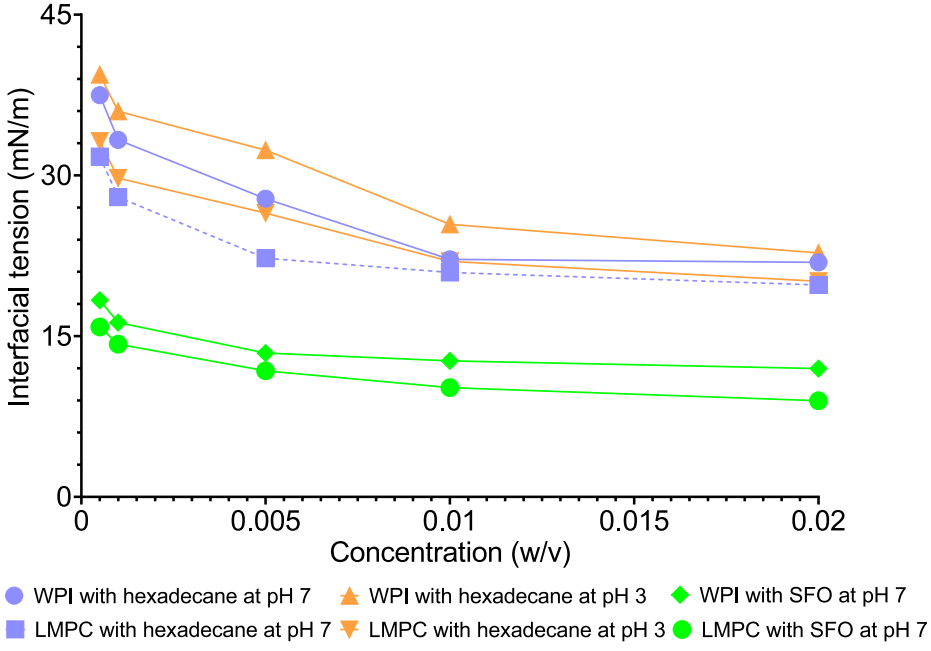

Fig. 5. Interfacial tension between hexadecane/SFO and WPI/LMPC solution at varying concentrations of proteins at pH = 3 and pH = 7. Error bars showing standard deviation cannot be seen since they are smaller than the symbol size (range of the standard deviation from 0.1 to 0.3 mN/m).

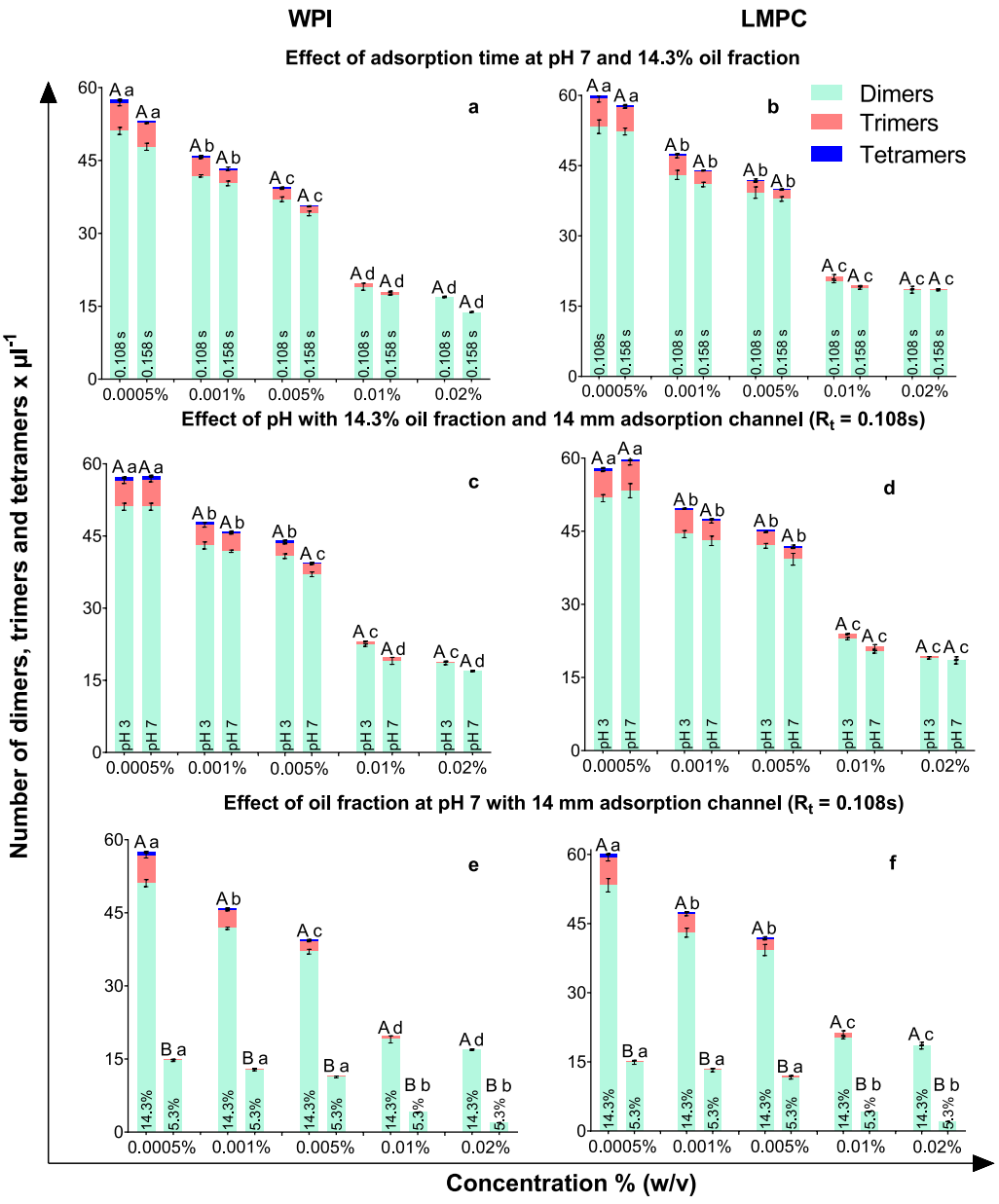

Fig. 6. Number of droplets undergoing coalescence at the start of the coalescence channel at different (a, b) adsorption time, (c, d) pH, and (e, f) oil fraction at different protein concentrations in emulsions prepared with hexadecane. Error bars show the standard deviation. Different capital letters mean significant differences ($p < 0.05$) in the effect of adsorption time/pH/oil fraction for a constant protein concentration and lowercase letters mean significant differences in the effect of protein concentration for a constant adsorption time/pH/oil fraction.

the protein concentration. While comparing the effect of adsorption time, pH and oil fraction, the maximum number of droplets undergoing coalescence is observed when the fraction of oil is at the highest value studied (14.3 % for hexadecane and 11.1% for SFO, Figure S2, Supplementary material). One-way ANOVA was conducted to assess the statistical significance of this effect and found that the increase in oil fraction has a significant impact on droplet coalescence. At a higher oil fraction, the flowrate lowers leading to an increase in the residence time that enables a higher number of collisions, leading to a higher rate of coalescence. Bigger droplets produced at higher oil fractions (Fig. 4) could have also had an impact on droplets undergoing a greater number of collisions and further getting coalesced. A significant difference in the number of droplets undergoing coalescence was also found while analyzing the effect of increase in protein concentration. Emulsions showed enhanced stability when the adsorption channel was longer, and pH was 7, regardless of the protein used for their stabilization. The behavior of SFO droplets was similar to that of hexadecane droplets, showing a notable increase in the number of droplets undergoing coalescence with increase in oil-fraction and protein concentrations (Figure S2). These findings have important implications for the design and optimization of microfluidic systems, particularly those involving emulsions, as they highlight the importance of considering the effects of oil-fraction, protein concentration, and pH on droplet behavior.

3.2. *Emulsion stability in the coalescence channel*

3.2.1. *Frequency of coalescence*

The frequency of coalescence (calculated with equation (2)) as a function of different concentrations of WPI and LMPC at varying oil fractions, pH, and adsorption times is plotted in Fig. 7 for hexadecane and SFO emulsions. It can be observed that the frequency of coalescence increased with the decrease in protein concentration. The increase in the frequency of coalescence is because of the low quantity of protein available to stabilize the oil droplets at the interface, which favors droplet coalescence when they collide. It can also be noted that several parameters affect the stability of the emulsion. When we look at the frequency of coalescence for a protein concentration of 0.02%, it can be observed that it increases when pH decreases from 7 to 3. This has to be

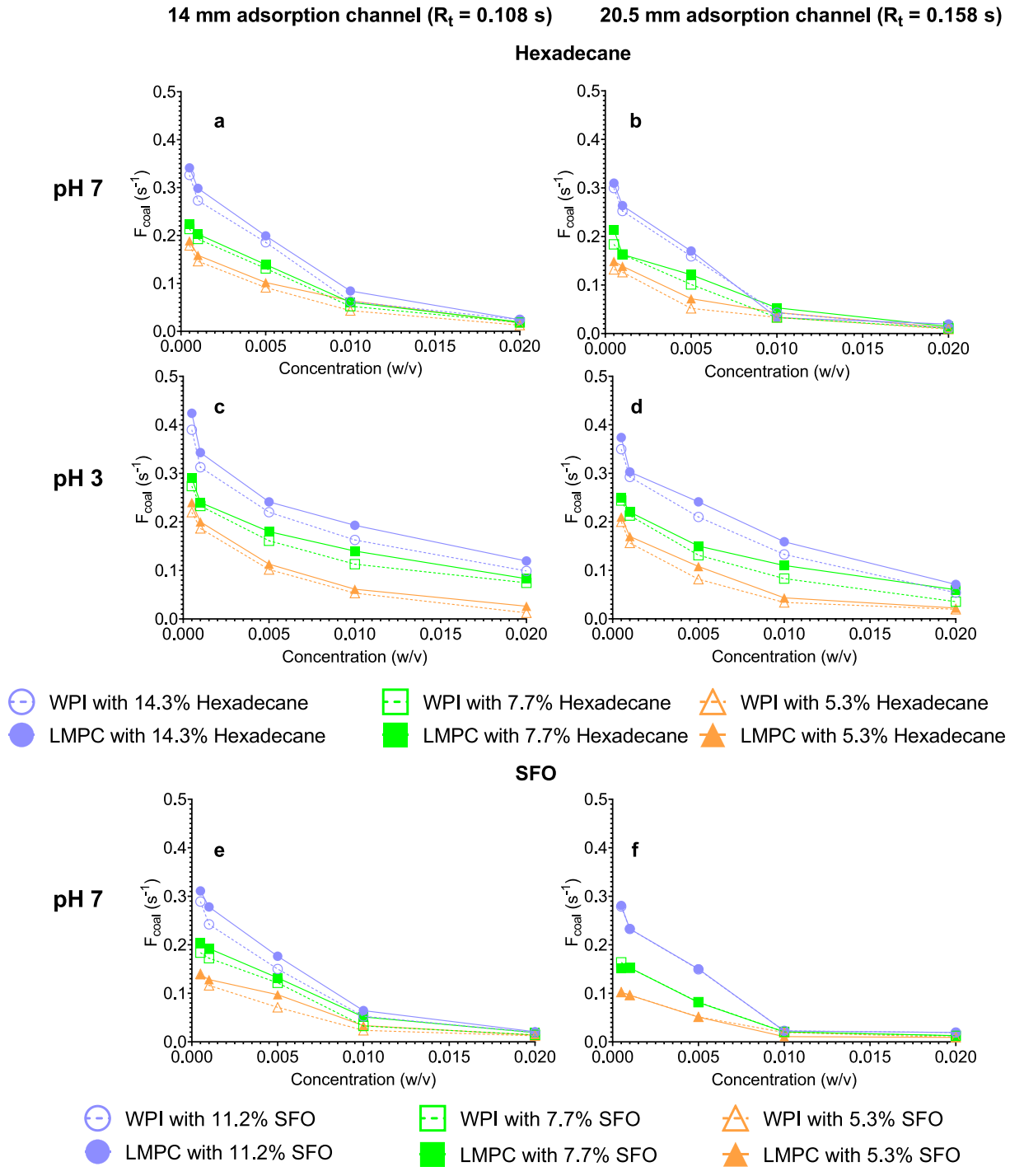

Fig. 7. Frequency of coalescence of emulsions stabilized with WPI and LMPC at different oils fractions and protein concentrations at (a) hexadecane, pH 7, and shorter adsorption time, 0.108 s; (b) hexadecane, pH 7, and longest adsorption time, 0.158 s; (c) hexadecane, pH 3, and shorter adsorption time, 0.108 s; (d) hexadecane, pH 3, and longest adsorption time, 0.158 s; (e) sunflower oil, pH 7, and shorter adsorption time, 0.108 s; (f) sunflower oil, pH 7, and longest adsorption time, 0.158 s. Error bars showing standard deviation cannot be seen since they are smaller than the symbol size.

related to the conformation changes that affect both WPI and LMPC, and that is more prominent for the highest oil fraction studied. Along with the protein concentration and pH, the fraction of oil plays also a significant role. Therefore, the frequency of coalescence was higher when the hexadecane fraction in the system was increased, the pH was low, and the adsorption time was short. Again, the values of the frequency of coalescence for both proteins are very similar (Fig. 7) and differences between them are not significant for the highest protein concentration.

While producing the emulsions with SFO, it was observed that these systems exhibit a similar trend as emulsions with hexadecane, but the frequency of coalescence was shown to be slightly lower, regardless of the protein, oil fraction, and adsorption time. The type of oil is one of the parameters which influences the protein interaction with the oil at the interface (Kalaydzhiev & Chalova, 2019). One of the stages that contribute to droplet coalescence is the thinning of the film between coalescing droplets (Narayan et al. 2020). The viscosity ratio between the discontinuous and continuous phases (μ_d/μ_c) is one of the parameters controlling the type of film formed between droplets. The higher the

viscosity ratio, the lower the deformability of the droplet approaching a situation of an immobile thin film that results in less coalescence. In this study, for the longest adsorption time, the frequency of coalescence at pH 7 (Fig. 7b and 7f) and low oil fractions, 5.3% and 7.7%, was significantly higher ($p < 0.05$, see supplementary material) for hexadecane when protein concentrations were below 0.01%. In our case, the viscosity ratios are about 3.5 and 32 for hexadecane and SFO, respectively, which could explain why for SFO the frequency of coalescence is slightly lower when not enough protein is available to stabilize the oil droplets. However, at the highest protein concentration, frequency of coalescence was close to zero regardless of the type of oil. While comparing the results between LMPC and WPI in terms of frequency of coalescence, it was proved that both proteins displayed similar results, particularly at pH 7, showing minor differences at pH 3. The impact of pH 3 on protein conformation and surface charge might be behind this behavior.

3.2.2. *Effect of protein concentration, adsorption time, and oil fraction on droplet coalescence*

By determining the number of dimers, trimers, and tetramers, it was possible to compare the formation of these droplets at the inlet and outlet of the coalescence channel. For hexadecane emulsions at pH = 7 and 14.3% oil fraction (Fig. 8), it can be observed that the number of trimers and tetramers formed reduces with the increase in protein concentration, regardless of the protein, with almost no trimers and tetramers formed at the highest protein concentration. At the lowest protein concentration, apart from the trimers and tetramers, the number of dimers formed also increases considerably near the outlet of the channel when compared to the inlet of the channel. But with the increase in the protein concentration, there is a reduction in the difference between the dimers formed at the outlet and inlet of the channel. Therefore, the increase of the protein concentration helps in protecting the droplets from undergoing coalescence, since it is feasible to assume that when the amount of protein in the system was not sufficient to completely adsorb on to the surface of the oil droplet (lowest protein concentrations) the oil droplets are more susceptible to coalescence. LMPC again shows a similar trend as WPI to stabilize these emulsions, however LMPC shows a slightly higher number of droplets undergoing coalescence at lower concentrations but is similar to WPI at higher concentrations of protein.

The formation of dimers also reduces with the increase in the protein adsorption time for the hexadecane and SFO emulsions (Figures 8 and S2, respectively). This indicates that increasing the contact time of oil droplets with the protein in the adsorption channel helps in better stabilizing of the oil droplets, since with higher adsorption times, there is more time for protein to be transported to the oil–water interface and hence stabilizing the oil droplet to a higher extent. Therefore, the number of droplets undergoing coalescence was lower at the start and end of the channel when a longer adsorption channel was used for both proteins.

However, when the protein concentration increases the number of coalesced droplets as a function of the adsorption time are very similar (Fig. 8), indicating that when the amount of protein present in the system is enough to stabilize the formed interfaces, there is a minor impact of the adsorption time, at least for the values studied in this work.

Oil fractions show to have a high impact on the frequency during which the droplets undergo coalescence. The number of droplets undergoing coalescence for hexadecane emulsions at pH 7 stabilized with WPI and LMPC at the start and the end of the coalescence channel for all the oil fractions studied (5.3, 7.7 and 14.3%) is plotted in Fig. 9. It is clear that the total number of droplets undergoing coalescence is more than 5 times at 14% oil fraction as compared to the emulsion with 5% oil fraction, regardless of the protein, and for the lowest protein concentration studied (0.0005%). With the increase in the oil fraction, the amount of protein available to be adsorbed on to the oil droplets is limited and hence increasing the chances of coalescence. But the reason why the formation of coalesced droplets is high at the highest oil fraction could also be ascribed to the lower total flowrate of the emulsion through the chip. As the emulsion has a higher residence time in the microchip, the chances of oil droplets colliding with each other

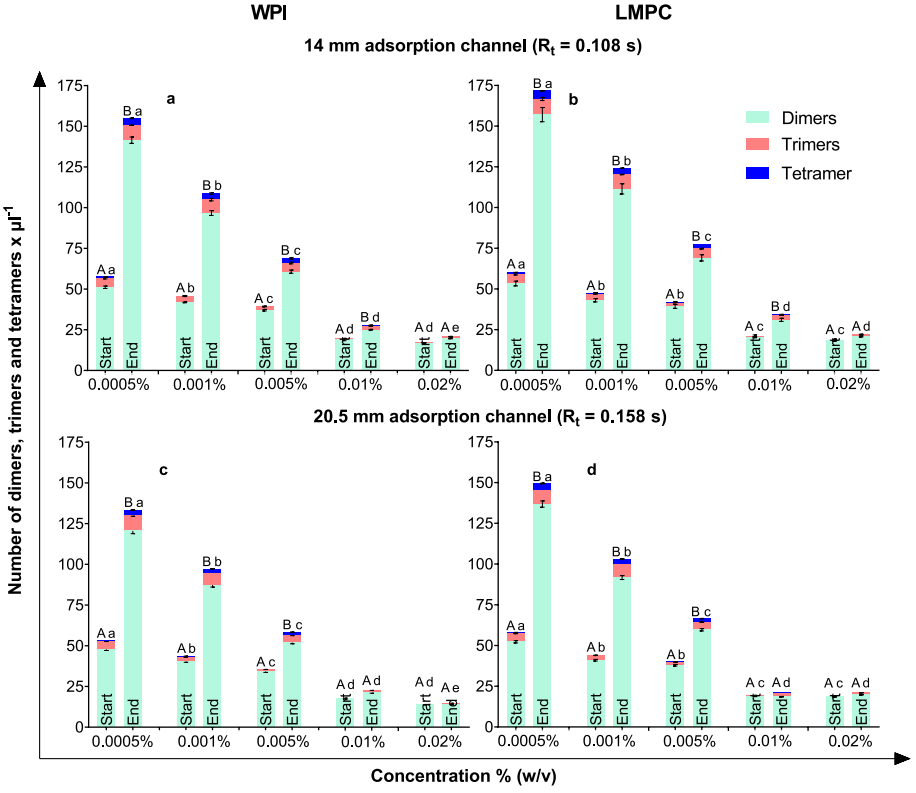

Fig. 8. Effect of protein concentration on the number of hexadecane droplets undergoing coalescence at the start and end of coalescence channel with 14.3% oil fraction for (a, b) adsorption times of 0.108 s (c, d) adsorption times of 0.158 s. Error bars show the standard deviation. Different capital letters mean significant differences ($p < 0.05$) in the number of droplets undergoing coalescence at the start and end of coalescence channel for a constant protein concentration and lowercase letters mean significant differences in the effect of protein concentration at the start/end of coalescence channel.

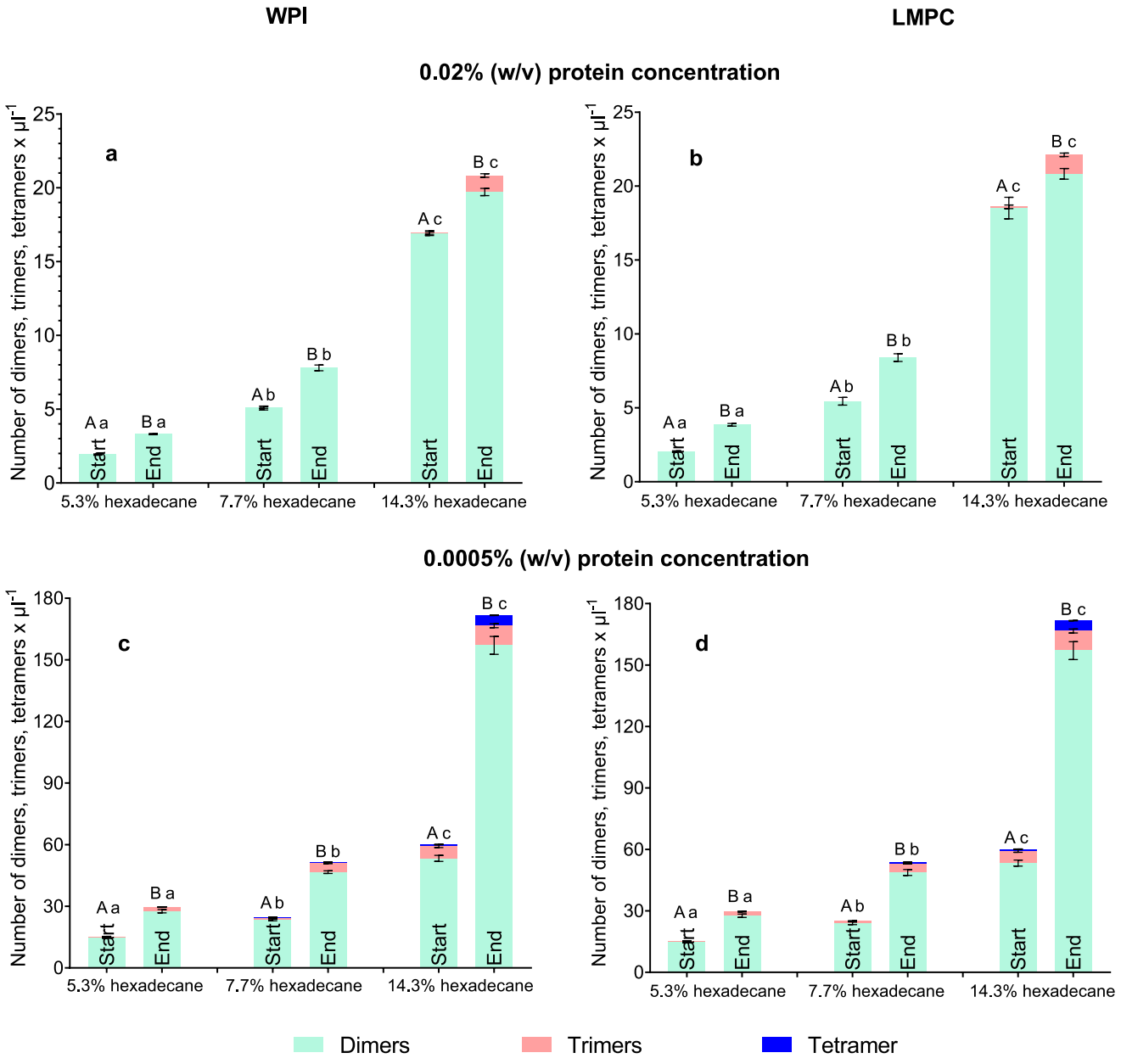

Fig. 9. Effect of hexadecane fraction on the number of droplets undergoing coalescence in the emulsions stabilized with (a, b) 0.02% and (c, d) 0.0005% WPI and LMPC using the chip of 0.108 s adsorption time. Error bars show the standard deviation. Different capital letters mean significant differences ($p < 0.05$) in the number of droplets undergoing coalescence at the start and end of coalescence channel at a constant oil fraction and lowercase letters mean significant differences in the number of droplets undergoing coalescence at different oil fractions at the start/end of coalescence channel.

increases, and hence leaving more room for droplets to undergo coalescence (Muijlwijk & Schroën, 2017). It should also be noted that the droplet size obtained was larger at a high oil fraction than that of the size of oil droplets at low oil fraction. The larger droplet size is another factor leading to an increase in the frequency of coalescence of droplets as there are higher chances of colliding with each other. Similar results (not shown) were obtained for emulsions prepared with SFO in the dispersed phase. The effect of interfacial tension and viscosity in droplet coalescence is discussed in the following section.

3.2.3. *Rate of formation of dimers and trimers*

The rate of formation of dimers and trimers gives the number of droplets undergoing coalescence per unit of volume and time (equation (3)).

$$\text{Rate of formation of dimers and trimers} = \frac{\text{Nie} - \text{Nis}}{\text{Rt}} \quad (3)$$

Where, Nie, and Nis are the number of dimers and trimers near the end and start of the coalescence channel respectively.

Fig. 10 gives the rate of formation of dimers and trimers while using the shortest adsorption time for the hexadecane and SFO at two oil fractions. As observed in the previous results, the increase in oil fraction has a high impact on the rate at which coalescence happens, mainly for dimer formation. While protein concentration and oil fraction affect the rate of dimer formation, it can be noted that the rate of formation of trimers is not so strongly affected by the increase of the oil fraction. The rate of trimer formation is between 4 and 6 trimers $\mu L^{-1}\, s^{-1}$ at the lowest protein concentration for both 5.3 and 14.3/11.7% oil fraction, while it is between 20 and 35 dimers $\mu L^{-1}\, s^{-1}$ and 30–100 dimers $\mu L^{-1}\, s^{-1}$ for

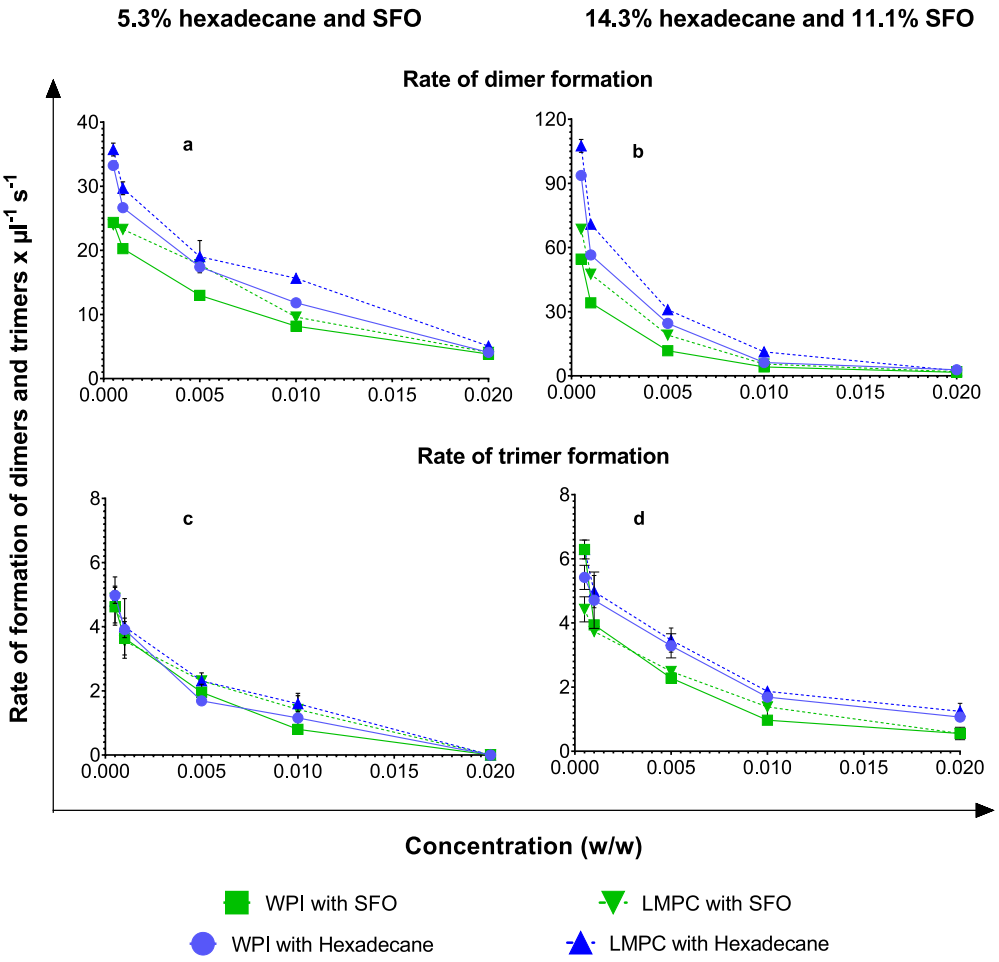

Fig. 10. Rate of formation of dimers and trimers at two different oil fractions in emulsions prepared with hexadecane and SFO with the shortest adsorption time (0.108 s), (a, c) 5.3% hexadecane and sunflower oil and (b, d) 14.3% hexadecane and 11.1% sunflower oil.

5.3 and 14.3/11.7% oil fraction, respectively, showing a clear influence of the oil content in the rate of coalescence.

At the same oil fraction, the difference in the rate of formation of dimers and trimers between SFO and hexadecane could be due to the difference in their physical properties, such as viscosity and interfacial tension. SFO has a higher viscosity and lower interfacial tension compared to hexadecane, which can lead to a more stable interface between the oil and water phases. Therefore, the type of oil used can have an effect on the stability of the emulsion and the rate of coalescence. As for the effect of the protein type, both WPI and LMPC seem to behave similarly regarding the rate of dimer and trimer formation.

3.2.4. Capillary number and rate of dimer formation

The characteristics of droplets in a multiphase system depend on various forces acting on them and the influence of these forces can be described using dimensionless numbers like Reynolds number (Re), Weber number (We), Bond number (Bo) and capillary number (Ca). For a microdroplet flow, it can be found that Re, We and Bo are small, which leads to a laminar flow where viscous forces and surface tension play a key role (Shen, Li, Liu, Cao, & Wang, 2015). Ca calculated using Equation (4) gives the ratio of viscous forces to surface tension.

$$\mathrm{Ca} = \frac{\mu U}{\sigma} \tag{4}$$

Where μ is the dynamic viscosity, U is the velocity and σ is the interfacial tension. Fig. 11 represents the correlation between the capillary number and the rate of dimer formation. The values used to calculate *Ca* are given in Tables S1 and S2 (Supplementary material).

According to (Ha, Yoon, & Leal, 2003), capillary number helps in determining the outcome of collisions between two droplets. The stability of droplets rises with an increase in the capillary number as the interfacial forces that maintain a drop's circular shape decrease with respect to the viscous forces that shear the droplet. When droplets are brought together in a shear flow, their interfaces flatten, and the droplets become deformable. Before the interfaces can get near enough for intermolecular interactions to become dominant and the interfaces to merge, the fluid film that forms between the droplets must drain. If the film does not thin enough during contact, the drops slide over one another, otherwise, they coalesce. Thus, droplets cannot coalesce when the capillary number is sufficiently high, and they coalesce when it is sufficiently low. The value below which there is droplet coalescence is known as the critical capillary number (Ca_c). When plotting the rate of dimer formation, the most prominent coalescence identified in the present study, versus the capillary number for the hexadecane and SFO emulsions stabilized with whey protein or LMPC, we can observe an exponential decay increasing Ca (Fig. 11). The rate of dimer formation increases sharply for $Ca < 0.02$ for the hexadecane emulsions, with coalescence values dropping and reaching the minimum values for $Ca > 0.02$, which may indicate this is the value of the Ca_c for hexadecane. For SFO emulsions, the exponential decay of the rate of dimer formation with the increase of Ca is also obtained for systems stabilized with whey protein of LMPC, with Ca_c of about 0.25–0.3.

As mentioned previously, for droplets to coalesce the film between them has to drain until the distance becomes small enough to cause its

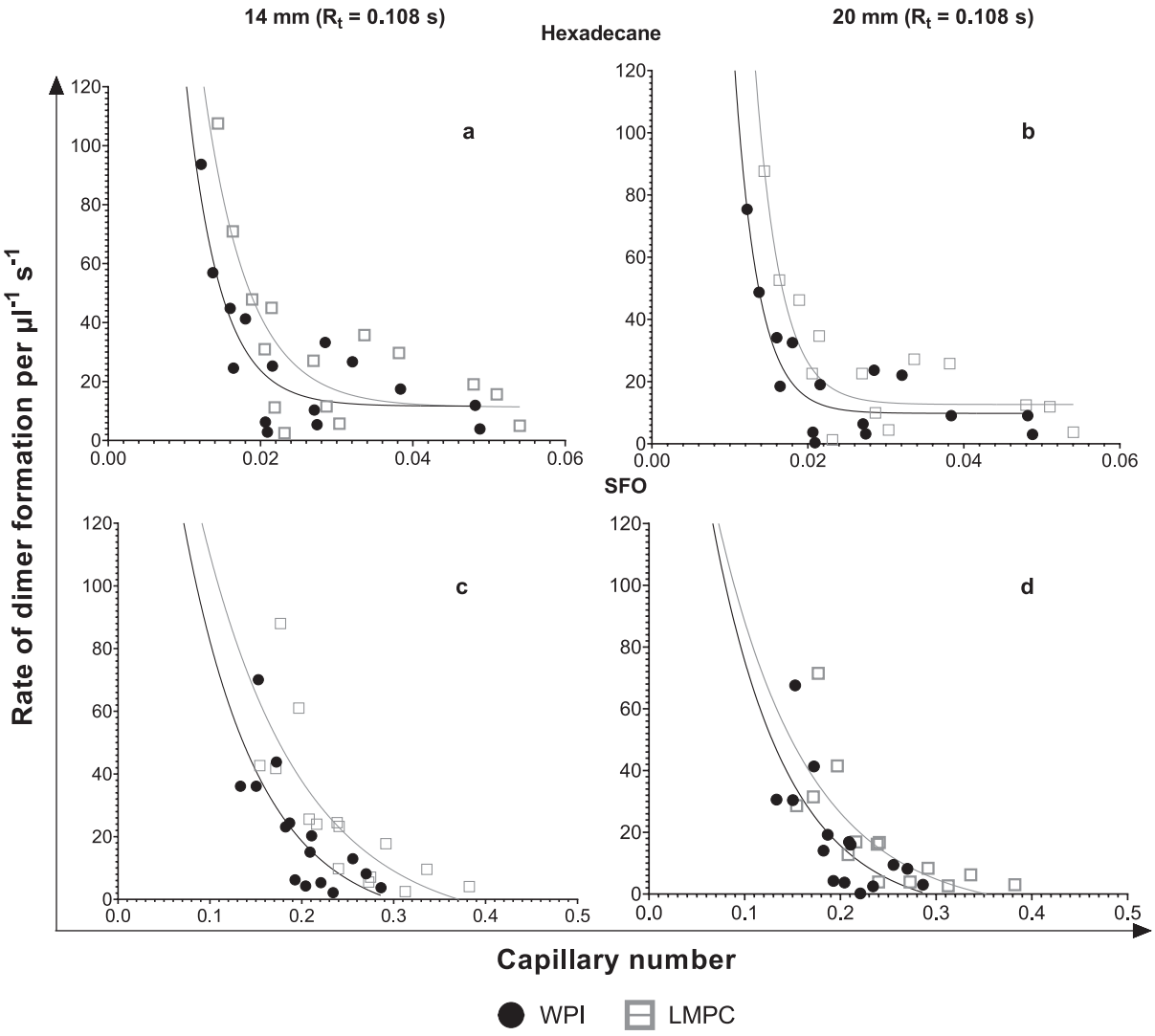

Fig. 11. Rate of formation of dimers against the capillary number with (a, b) 14.3% hexadecane and (c, d) 11.1% SFO stabilized with WPI and LMPC (0.0005–0.02%) with chips of 0.108 s adsorption time (a, c) and 0.158 s adsorption time (b, d).

rupture. The film drainage time (T_d) can be calculated using Equation (5), as described by Shen et al., for the hexadecane and SFO emulsions stabilized with whey protein and LMPC at pH 7.

$$\mathrm{Td} = 40\,\mathrm{r}\sqrt{\frac{\mu}{\sigma U}} \tag{5}$$

where r is the radius of the droplets.

The film drainage time increases with the capillary number (Fig. 12) which can be explained considering that at higher capillary numbers there is an increase in the radius of the thin film formed between the droplets. Since film drainage is the result of the pressure gradient, that is inversely proportional to the radius of the thin film, this situation will lead to longer film drainage times (Narayan, Metaxas, Bachnak, Neumiller, & Dutcher, 2020). Moreover, the presence of the proteins in the interface are responsible for decreasing coalescence. It is assumed that during film thinning, the surfactant is drawn along the film boundaries, creating an interfacial tension gradient. As a result, Marangoni flow rises and tends to oppose film drainage. In the present study, very similar film drainage times are obtained for LMPC stabilized emulsions compared with the ones from whey protein emulsions. As for the effect of the type of oil in the film drainage time, the higher values of the film drainage time obtained for the SFO emulsions correlate with the lower values of the frequency of coalescence (Fig. 7) and rate of dimer formation (Fig. 10) already shown.

4. Conclusions

The research clearly shows that lesser mealworm protein concentrate, a protein from a more sustainable source, is able to stabilize hexadecane and sunflower oil emulsions similarly than whey protein. Using a microfluidic system to produce emulsions under controlled conditions and a costume-build methodology of image acquisition and analysis, it was possible to account for droplet coalescence both at the beginning and at the end of the coalescence channel. The methodology enables to distinguish between single droplets and dimers, trimers, and tetramers formed as a result of droplet coalescence, allowing to calculate the frequency of coalescence and also the rate of formation for each type of droplet. Droplet coalescence was maximum, regardless of the protein, at the lowest protein concentration (0.0005%), shorter adsorption time (0.04 s), lowest pH (3), and highest oil fraction, 14.3% for hexadecane and 11.2% for sunflower oil. Stability of emulsions increased at pH = 7 and with the increase in protein concentration, adsorption time, and reduction in oil-fraction. In terms of the main parameters of the process, oil-fraction had the highest impact on droplet coalescence. The increase

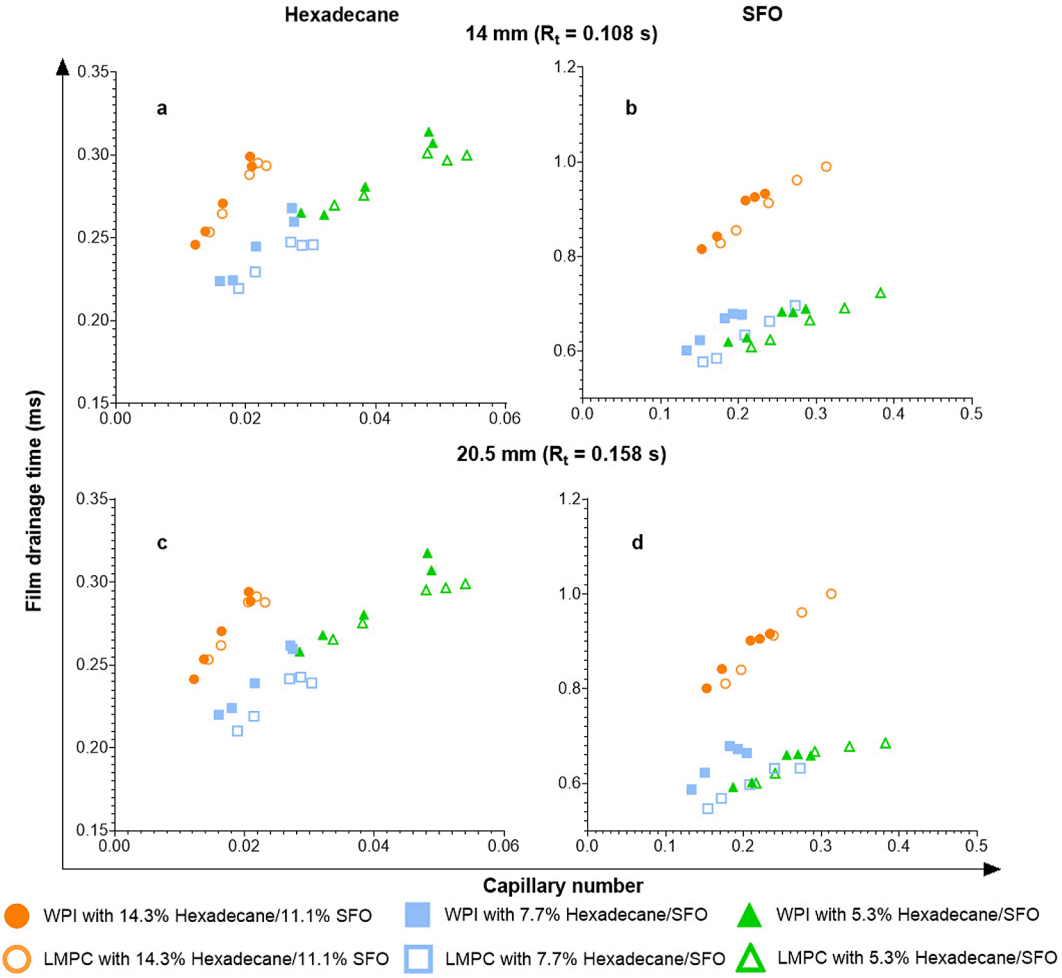

Fig. 12. Film drainage time at different protein concentrations as a function of capillary number at different oil fractions of (a, b) hexadecane and (b, d) SFO (b, d) at two different adsorption times of 0.108 s (a, b) and 0.158 s (c, d).

in oil fraction resulted in a substantial increase in droplet diameters, which in turn led to an increase in coalescence, since bigger droplets have a higher probability of colliding and merging. SFO, with a higher viscosity and lower interfacial tension, resulted in smaller droplets than hexadecane, with a slightly lower frequency of coalescence, which agree with the higher values of the film drainage time obtained for this oil. Protein concentration had higher impact on the droplet stability than the type of the protein source (WPI vs. LMPC), with a decrease in protein concentration leading to an increase in coalescence. Dimer formation has been identified as the main coalescence event taking place in the model and food-grade oil emulsions regardless of the protein used for stabilization. Moreover, the rate dimer formation decreases increasing Ca allowing to determine the value of the critical capillary number for each system which is highly influenced by the viscosity of the oil phase. Lesser meal worm protein concentrate has been proven to stabilize emulsions similarly to whey protein under controlled conditions and can be therefore used in food preparations that will benefit from using more sustainable ingredients.

CRediT authorship contribution statement

Jitesh Jayakumar: Conceptualization, Methodology, Investigation, Writing – original draft. **Aurélie Ballon:** Investigation. **Jordi Pallarès:** Software, Funding acquisition. **Anton Vernet:** Software, Funding acquisition. **Sílvia de Lamo-Castellví:** Conceptualization, Funding acquisition. **Carme Güell:** Conceptualization, Writing – review & editing, Supervision, Funding acquisition. **Montserrat Ferrando:** Conceptualization, Writing – review & editing, Supervision, Funding acquisition.

Declaration of Competing Interest

The authors declare that they have no known competing financial interests or personal relationships that could have appeared to influence the work reported in this paper.

Data availability

Data will be made available on request.

Acknowledgement

This project was financially supported by the fundings from European Union Horizon 2020 research and innovation programme under Marie Sklodowska-Curie grant agreement No 713679 and from the Universitat Rovira i Virgili (URV), and Ministerio de Economia y Competitividad PGC 2018-097095-B-I00. J. P. and A. V acknowledge the support of the Ministerio de Ciencia, Innovación y Universidades through the grant RTI2018-100907-A-I00 (MCIU/AEI/FEDER) and by the Generalitat de Catalunya through the grant 2017-SGR-1234.

We would also like to extend our sincere appreciation to Salvatore Cito for his invaluable assistance and contribution to the successful completion of the experiments and the overall project.

Appendix A. Supplementary data

Supplementary data to this article can be found online at https://doi.org/10.1016/j.foodres.2023.113100.

References

Akkaya, M. R. (2018). Prediction of fatty acid composition of sunflower seeds by near-infrared reflectance spectroscopy. *Journal of Food Science and Technology, 55*(6), 2318–2325. https://doi.org/10.1007/s13197-018-3150-x

Bera, B., Khazal, R., & Schroën, K. (2021). Coalescence dynamics in oil-in-water emulsions at elevated temperatures. *Scientific Reports, 11*(1), 1–10. https://doi.org/10.1038/s41598-021-89919-5

Camin, D. L., Forziati, A. F., & Rossini, F. D. (1964). Physical properties of n-Hexadecane, n-Decylcyclopentane, 12-Decylcyclohexane, I-Hexadecene and n-Decylbenzene'. *The Journal of Physical Chemistry, 613*(8), 440–442.

Dudek, M., Fernandes, D., Helno Herø, E., & Øye, G. (2020). Microfluidic method for determining drop-drop coalescence and contact times in flow. *Colloids and Surfaces A: Physicochemical and Engineering Aspects, 586*. https://doi.org/10.1016/j.colsurfa.2019.124265

Gould, J., & Wolf, B. (2018). Interfacial and emulsifying properties of mealworm protein at the oil/water interface. *Food Hydrocolloids, 77*, 57–65. https://doi.org/10.1016/j.foodhyd.2017.09.018

Güell, C., Ferrando, M., Trentin, A., & Schroën, K. (2017). Apparent Interfacial Tension Effects in Protein Stabilized Emulsions Prepared with Microstructured Systems. *Membranes, 7*(19), 5–7. https://doi.org/10.3390/membranes7020019

Ha, J. W., Yoon, Y., & Leal, L. G. (2003). Simulation of droplet coalescence in simple shear flow. *Physics of Fluids, 15*(4), 849–867. https://doi.org/10.1063/1.1555803

Henchion, M., Hayes, M., Mullen, A. M., Fenelon, M., & Tiwari, B. (2017). Future protein supply and demand: Strategies and factors influencing a sustainable equilibrium. *Foods, 6*(7), 1–21. https://doi.org/10.3390/foods6070053

Hinderink, E. B. A., Kaade, W., Sagis, L., Schroën, K., & Berton-Carabin, C. C. (2020). Microfluidic investigation of the coalescence susceptibility of pea protein-stabilised emulsions: Effect of protein oxidation level. *Food Hydrocolloids, 102*. https://doi.org/10.1016/j.foodhyd.2019.105610

Ho, T. M., Razzaghi, A., Ramachandran, A., & Mikkonen, K. S. (2022). Emulsion characterization via microfluidic devices: A review on interfacial tension and stability to coalescence. *Advances in Colloid and Interface Science*, *299*(October 2021), 102541. https://doi.org/10.1016/j.cis.2021.102541.

Huang, D., & Meng, T. (2020). Precise control for the size of droplet in T-junction microfluidic based on iterative learning method. *Journal of the Franklin Institute, 357*(9), 5302–5316. https://doi.org/10.1016/j.jfranklin.2020.02.046

Jafari, S. M., Assadpoor, E., He, Y., & Bhandari, B. (2008). Re-coalescence of emulsion droplets during high-energy emulsification. In. *Food Hydrocolloids* (Vol. 22, Issue 7). https://doi.org/10.1016/j.foodhyd.2007.09.006

Kalaydzhiev, H., & Chalova, V. I. (2019). Stability of sunflower and rapeseed oil-in-water emulsions supplemented with ethanol-treated rapeseed meal protein isolate. *Journal of Food Science and Technology, 56*(6), 3090–3098. https://doi.org/10.1007/s13197-019-03806-6

Kim, T. K., & Choi, Y. S. (2021). Physicochemical and textural properties of emulsions prepared from the larvae of the edible insects Tenebrio molitor, Allomyrina dichotoma, and Protaetia brevitarsis seulensis. *Journal of Animal Science and Technology, 63*(2), 417–425. https://doi.org/10.5187/JAST.2021.E25

Maan, A. A., Nazir, A., Khan, M. K. I., Boom, R., & Schroën, K. (2015). Microfluidic emulsification in food processing. In *Journal of Food Engineering* (Vol. 147, pp. 1–7). Elsevier Ltd. https://doi.org/10.1016/j.jfoodeng.2014.09.021.

McClements, D. J. (2004). Protein-stabilized emulsions. *Current Opinion in Colloid and Interface Science, 9*(5), 305–313. https://doi.org/10.1016/j.cocis.2004.09.003

McClements, D. J. (2016). *Food Emulsions ultima versión (Third edit)*. CRC Press.

Mintah, B. K., & Ma, H. (2020). Edible insect protein for food applications: Extraction, composition, and functional properties. *Journal of Food Process Engineering, 43*(4), 1–12. https://doi.org/10.1111/jfpe.13362

Mishyna, M., Martinez, J. J. I., Chen, J., & Benjamin, O. (2019). Extraction, characterization and functional properties of soluble proteins from edible grasshopper (Schistocerca gregaria) and honey bee (Apis mellifera). *Food Research International*, *116*(April 2018), 697–706. https://doi.org/10.1016/j.foodres.2018.08.098.

Muijlwijk, K., & Schroën, K. (2017). Coalescence of protein-stabilised emulsions studied with microfluidics. *Food Hydrocolloids, 70*, 96–104.

Narayan, S., Metaxas, A. E., Bachnak, R., Neumiller, T., & Dutcher, C. S. (2020). Zooming in on the role of surfactants in droplet coalescence at the macroscale and microscale. *Current Opinion in Colloid and Interface Science, 50*, Article 101385. https://doi.org/10.1016/j.cocis.2020.08.010

Narsimhan, G., & Goel, P. (2001). Drop coalescence during emulsion formation in a high-pressure homogenizer for tetradecane-in-water emulsion stabilized by sodium dodecyl sulfate. *Journal of Colloid and Interface Science, 238*(2), 420–432. https://doi.org/10.1006/jcis.2001.7548

Okushima, S., Nisisako, T., Torii, T., & Higuchi, T. (2004). Controlled production of monodisperse double emulsions by two-step droplet breakup in microfluidic devices. *Langmuir, 20*(23), 9905–9908. https://doi.org/10.1021/la0480336

Rumpold, B. A., & Schlüter, O. K. (2013). Potential and challenges of insects as an innovative source for food and feed production. *Innovative Food Science and Emerging Technologies, 17*, 1–11. https://doi.org/10.1016/j.ifset.2012.11.005

Shen, F., Li, Y., Liu, Z. M., Cao, R. T., & Wang, G. R. (2015). Advances in Micro-Droplets Coalescence Using Microfluidics. *Chinese Journal of Analytical Chemistry, 43*(12), 1942–1954. https://doi.org/10.1016/S1872-2040(15)60886-6

Tcholakova, S., Denkov, N. D., & Banner, T. (2004). Role of surfactant type and concentration for the mean drop size during emulsification in turbulent flow. *Langmuir, 20*(18), 7444–7458. https://doi.org/10.1021/la049335a

Wang, J., Ballon, A., & Güell, C. (2021a). Polyphenol loaded w1/o/w2 emulsions stabilized with lesser mealworm (Alphitobius diaperinus) protein concentrate produced by membrane emulsification: Stability under simulated storage, process, and digestion conditions. *Foods, 10*(12), 2997. https://doi.org/10.3390/foods10122997

Wang, J., Jousse, M., & Güell, C. (2021b). Black soldier fly (Hermetia illucens) protein concentrates as a sustainable source to stabilize o/w emulsions produced by a low-energy high-throughput emulsification technology. *Foods, 10*(5). https://doi.org/10.3390/foods10051048

Watanabe, T., Kawai, T., & Nonomura, Y. (2018). Effects of fatty acid addition to oil-in-water emulsions stabilized with sucrose fatty acid ester. *Journal of Oleo Science, 67*(3), 307–313. https://doi.org/10.5650/jos.ess17097

Xu, J. H., Li, S. W., Tan, J., Wang, Y. J., & Luo, G. S. (2006). Preparation of Highly Monodisperse Droplet in a T-Junction Microfluidic Device. *AIChE Journal, 52*(9), 3005–3010.

Yi, L., & Boekel, M. A. J. S. V. (2013). Extraction and characterisation of protein fractions from five insect species. *Food Chemistry, 141*(4), 3341–3348. https://doi.org/10.1016/j.foodchem.2013.05.115

Yonguep, E., Kapiamba, K. F., Kabamba, K. J., & Chowdhury, M. (2022). Formation, stabilization and chemical demulsification of crude oil-in-water emulsions: A review. *Petroleum Research, 7*(4), 459–472. https://doi.org/10.1016/j.ptlrs.2022.01.007